The Visual Computer

Achieving developability of a polygonal surface by minimum deformation: a study of global and local optimization approaches

Charlie C.L. Wang[1], Kai Tang[2]

[1] Department of Automation and Computer-Aided Engineering, The Chinese University of Hong Kong, Shatin, N.T., Hong Kong
E-mail: cwang@acae.cuhk.edu.hk
[2] Department of Mechanical Engineering, Hong Kong University of Science and Technology, Clear Water Bay, N.T., Hong Kong
E-mail: mektang@ust.hk

Published online: 15 September 2004

Surface developability is required in a variety of applications in product design, such as clothing, ship hulls, automobile parts, etc. However, most current geometric modeling systems using polygonal surfaces ignore this important intrinsic geometric property. This paper investigates the problem of how to minimally deform a polygonal surface to attain developability, or the so-called developability-by-deformation problem. In our study, this problem is first formulated as a global constrained optimization problem and a penalty-function-based numerical solution is proposed for solving this global optimization problem. Next, as an alternative to the global optimization approach, which usually requires lengthy computing time, we present an iterative solution based on a local optimization criterion that achieves near real-time computing speed.

Key words: Developable surface – Polygonal mesh – Assembled patches – Deformation – Optimization

Correspondence to: C.C.L. Wang

1 Introduction

Developability is an important intrinsic property of a surface. Informally, a surface is developable if it can be flattened onto a plane without any distortion [1]. This is a highly desired property in sheet manufacturing industry, where the stretch or compression in the sheet material should be avoided, as they make the product more prone to damage since internal strains and stresses are generated. As an example (Fig. 1a), the original design of the shell has a developable shape that can be bent or rolled by a metal sheet. After being deformed by "Wires" [2], its shape becomes the one shown in Fig. 1b, which is non-developable. The elastic energy maps of the shell surface before and after the deformation are given in Fig. 1c and 1d, respectively. As clearly shown, a great amount of elastic energy is generated if the newly designed shell is to be manufactured by the metal sheet. This requirement exists in many applications (e.g., clothing, ship hulls, ducts, shoes, aircraft and automobile parts). In this paper, we investigate and propose algorithms for solving the problem of how to deform a non-developable surface, in the form of assembled polygonal mesh patches, into a developable one while at the same time minimizing the difference between the two surfaces.

Our algorithms work on polygonal mesh patches, which have become a widely accepted standard in most computer graphics applications. Triangular meshes are especially preferred due to their algorithmic simplicity, numerical robustness, and efficient display. The advantage of switching from spline-based surface representation to mesh representation is mainly due to the fact that algorithms for polygonal meshes usually can work on shapes with arbitrary topology and do not suffer from the severe restrictions that stem from the rigid algebraic structure of polynomial surfaces. More and more commercial modeling systems have included the polygonal mesh-based module, and more and more applications are developed based on mesh representation.

The proposed technique is new; no prior research on developability optimization of polygonal surfaces has been found in the literature. In our approach, the surface developability problem is formulated as a constrained optimization problem. The problem is first solved numerically by a penalty function-based optimization scheme, which is a global approach. The continuity is preserved between the assembled patches. The global optimization is very time-consuming even after the gradients of the objective function have already been calculated locally.

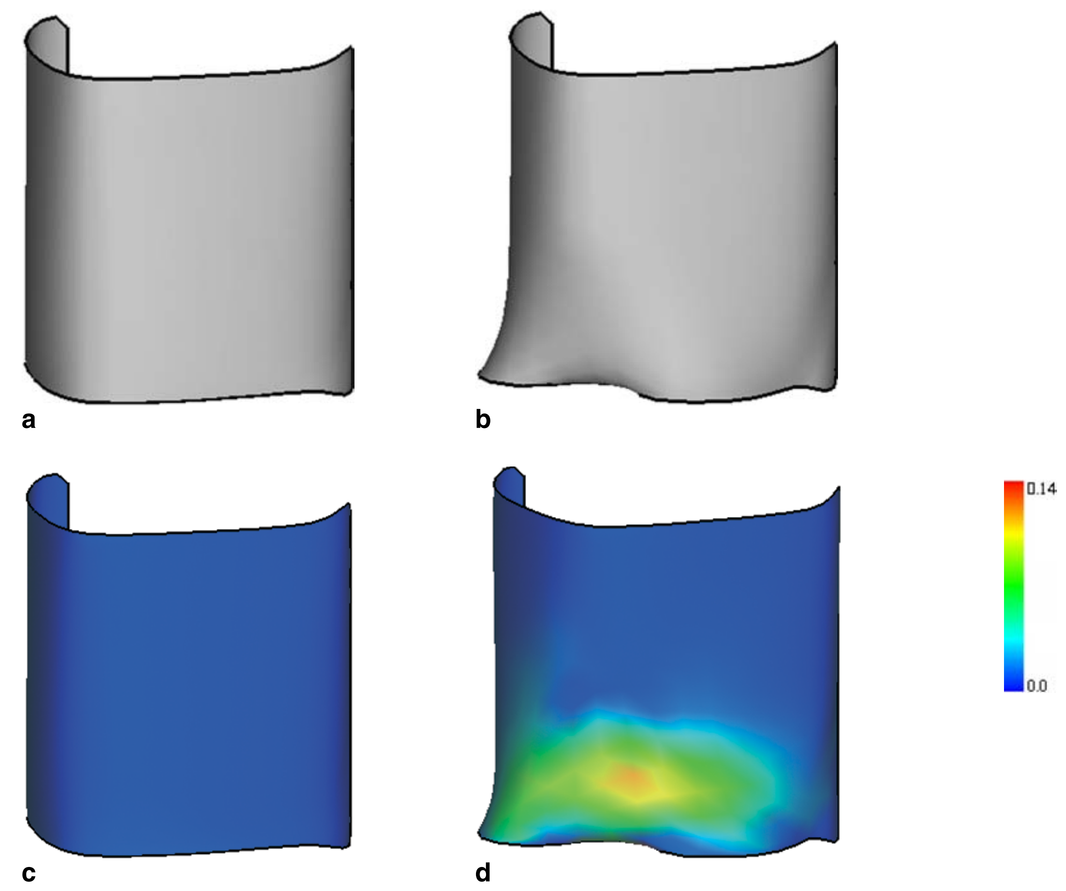

Fig. 1a–d. Example I. A deformed shell leads to stretch in manufacturing: **a** Original shape **b** Deformed shape **c** Elastic energy map of the original duct **d** Elastic energy map of the newly shaped duct

Therefore, as an alternative, we further present a local optimization solution in which the vertices on the surface are moved along their normal directions iteratively. The magnitude of each movement is actually derived from a locally defined objective function. This local approach enjoys a great advantage of faster computing speed as compared to its global counterpart and can be integrated into modeling systems to preserve the developability of assembled surface patches in real-time during the entire design process. Different from most existing surface modeling solutions concerned with developability, our solutions, both global and local approaches, are more of a bottom-up nature – we take as input an arbitrary (non-developable) surface in the form of a set of assembled polygonal mesh patches and output a *developable* polygonal mesh that deviates minimally from the original surface.

The paper is organized as follows. After reviewing the related work, the necessary mathematical formulations about the developability of a polygonal mesh are given in Sect. 3, where the developability-by-deformation problem is formulated as a constrained optimization problem. In Sect. 4, the details of a penalty-function-based solution are presented that numerically solves this constrained optimization problem. To overcome the usually lengthy computing time required by the proposed numerical solution, as an alternative, in Sect. 5 we reformulate the problem as a local optimization problem and propose a much quicker numerical algorithm to solve the local optimization problem. In Sect. 6 we then provide some experimental examples to illustrate the functionality of the proposed solutions as well as their comparison. Finally, the paper is concluded in Sect. 7 and we offer some pointers to potential future research in this area.

2 Related work

Over the past decade, mesh-processing techniques, such as mesh simplification [3–5] and mesh fairing [6–10], have been improved significantly. Apart from fundamental mesh processing algorithms, many new freeform modeling approaches have also been developed. The SKETCH system [11] rapidly constructs an approximate shape via direct mark-based interaction. The Teddy system [12] constructs a rounded freeform mesh model by finding the chordal-axis of the user input 2D closed stroke to build a smooth surface around the axis. Other approaches construct mesh surfaces by use of implicit surfaces [13, 14]. Suzuki et al. [15] presented a 3D mesh-dragging method for intuitive, efficient geometric modeling of free-form polygonal models; this method is based on an adaptive remeshing procedure. With their method, the user can drag a part of a triangular mesh and change its position and orientation. Other interactive modeling research results were reported for the multi-resolution presentation of models. For example, Zorin et al. [16] built a scalable interactive multi-resolution editing system based on mesh refinement and coarsification algorithms, and based on Zorin's approach Khodakovsky and Schroder [17] developed an algorithm that can modify the fine level shape of a surface. However, in all the above approaches, the developability of the processed polygonal mesh surface is not considered. Our paper considers the developability property of the given polygonal surface and converts the original non-developable surface into a developable one.

Developable surfaces have been studied for a long time. The definition of a developable surface ([1]) is derived from a ruled surface. For a ruled surface, $X(t, v) = \alpha(t) + v\beta(t)$, it is developable if β, $\frac{d\beta}{dt}$ and $\frac{d\alpha}{dt}$ are coplanar for all points on X (where $\alpha(t)$ is the *base curve* and $\beta(t)$ is the *director curve* of $X(t, v)$). The simplest examples of developable surfaces are cylinders and cones, and a simple and representative example of non-developable surfaces is a sphere. Every surface enveloped by a one-parameter family of planes is a developable surface. The key concept in characterizing the developability is Gaussian curvature, which is the product of the maximum and minimum normal curvatures at a given point [1]. In general, a surface is developable if and only if the *Gaussian curvature* of every point on it is zero. This is the constraint that we want to preserve during the surface optimization. Research related to computer-aided geometric design, in particular those concerning the design and approximation of developable surfaces, can be found in [18–27]. Most of them are in terms of NURBS or its special case B-spline or Bézier surfaces [18–24]. Aumann [18] proposed the condition under which a developable Bézier surface can be constructed with two boundary curves. The boundary curves in his approach are restricted to lie in parallel planes; the projection of the boundary curves on the xy plane must be a rectangle. Chalfant and Maekawa [19] presented a method to design developable B-spline surfaces where boundary curves do not necessarily lie in parallel planes. In the work of Frey and Bindschadler [20], the results of Aumann are extended by generalizing the degree of the directions. Their system requires solving a nonlinear system of equations to find the Bézier control points. Chu and Séquin [21] recently proposed a new method to design a developable Bézier patch. In their method, after one boundary curve is freely specified, five more degrees of freedom are available for a second boundary curve of the same degree. In the work of [22–24], approximation methods are used to design developable B-spline surfaces based on projective geometry. Other approaches are based on alternative perspectives. Redont [25] constructed developable surfaces by specifying tangent planes along a geodesic of a surface, Randrup [26] approximated a given surface by cylinders in its Gaussian image, and Park et al. [27] designed developable surfaces by the methods from optimal control theory.

All the work in the above references tried to use developable surfaces to (approximately) construct the shape of a product. There are also some surface flattening approaches [28–37] in literature. They usually adopt nonlinear programming techniques to find an optimized flattened result with respect to the given 3D surface. Shimada and Tada [28] presented a generic surface development algorithm. This algorithm is based on a meshed surface. In their algorithm, a dynamic programming method is used to develop a curved surface. An objective curved surface is decomposed into regions of adjacent strips. Then each region is developed, in turn, into a flattened shape. The whole shape is derived by solving a multi-stage decision process. Parida and Mudur [29] gave an algorithm to develop complex surfaces. Their algorithm first obtains an approximate planar surface, and then reorients cracks and overlapping parts in the developed plane to satisfy orientation constraints. The algorithm of Parida and Mudur might generate many cracks and calculation errors. McCartney et al. [30] flatten a triangulated surface by minimizing the strain energy in the 2D pattern. The surface is first triangulated using Delaunay triangulation. Then the triangles are transformed onto a 2D plane. However, there are some flattened triangles that cannot preserve their length relationship with respect to the triangles on the surface. These length differences are measured as strain energy. If the strain energy is zero, that means the flattened triangles preserve their length relationships with the original triangles on the surface, i.e., no deformation occurs. Thus, an iterative method is applied to minimize this strain energy in the 2D pattern. The endpoints of the triangles are moved in orthogonal directions by trial to obtain smaller energy in each iteration. Wang et al. [31] improve McCartney's algorithm by using a spring-mass system. This guides the endpoints to approach better positions by the force of springs and the computational speed of the minimization is improved. The accuracy of the flattening can also be controlled by using the spring constant. Sheffer and de Sturler [33, 34] presented a texture mapping algorithm that causes small mapping distortion. Their algorithm consists of two steps: (1) Using the angle based flattening (ABF) parameterization method to provide a continuous (no foldovers) mapping, which concentrates on minimizing the angular distortion of the mapping so leads to relatively large linear distortion; and (2) To reduce the linear distortion, an inverse mapping from the plane to the result of ABF is computed to improve the parameterization – the improved result has low length distortion. The methods presented in [38, 39] handle the problem in a reverse way by fitting a 2D patch onto a 3D surface. However, even if an optimized flattened 2D shape is obtained, warping a sheet of such a 2D shape into the given 3D shape usually leads to stretching if the given surface itself is non-developable. Therefore, the essential solution is to let the surface itself be developable.

As alluded to earlier, we propose to convert the Gaussian curvature of every point on the assembled mesh patches to zero during an optimization process. However, since differential geometry analyzes surfaces in the continuum domain, the traditional equations for calculating the Gaussian curvature cannot be applied to a mesh surface directly. A discrete Gaussian curvature computing method is needed. After Calladine (1984) firstly formulated the discrete Gaussian curvature in [40], Kobbelt et al. [41] gave the formulas of discrete Gaussian curvature based on the fact that a mesh can be interpreted as an approximation of a smooth surface. The idea in [41] is to discretize the formulation for defining the Gaussian curvature on a smooth surface based on a theorem by Rodrigues [1]. In a similar way, Sheffer [42] gave another discrete Gaussian curvature approximation, which is scale independent. In our approach, we utilize the formula of Kobbelt et al. [41] to derive the developability of a polygonal mesh surface.

3 Mathematical formulation

This section gives the necessary mathematical formulation based on which our optimization algorithms will be developed.

3.1 Representation of assembled polygonal patches

A polygonal patch M is defined as a pair (K, V), where K is a simplicial complex specifying the connectivity of the vertices, edges, and faces (in other words, the topological graph of M), and $V = \{v_1, \cdots, v_m\}$ is the set of vertices defining the shape of the polyhedral patch in $\Re^3$. The above definition follows the notation in [43]. In this paper, to simplify the algorithm, every polygonal face in M is subdivided into triangles by the *constrained Delaunay triangulation* (CDT) [44] of a planar contour. If the contour of a polygonal face is not coplanar, we project the vertices of this face onto its least-square plane to apply the CDT. No new vertex is inserted and the triangulation on the vertices before projection can be obtained by maintaining the same connectivity of CDT result on the least-square plane. From K, it is straightforward for our algorithm to fetch the adjacent nodes, edges, and faces of a triangular node in constant time. The object considered in our approach is denoted by O which is a collection of assembled polygonal patches M_i, i.e., $O = M_1 \cup M_2 \cup \cdots \cup M_m$. Each surface patch

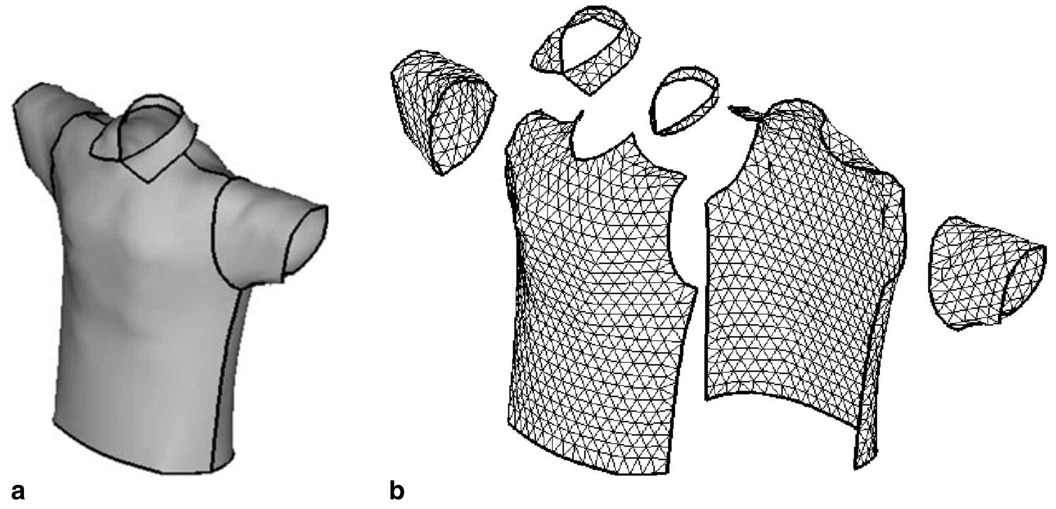

Fig. 2a,b. Assembled polygonal surface patches.: **a** Assembled surface patches **b** Mesh representation of each patch

M_i is a two-manifold in the form of a piecewise linear triangular mesh. The given polygonal patches are usually assembled together by sharing some common triangular edges (as illustrated in Fig. 2). In the following, the developability of a polygonal patch is first studied locally, and then its global developability function is defined.

3.2 Developability of a polygonal mesh patch

By theorems from differential geometry, one can easily detect whether a surface is developable according to its overall Gaussian curvature [1]: "The Gaussian curvature of a developable surface is identically *zero* at every regular point." However, Gaussian curvature is not well defined mathematically on a piecewise linear polygonal mesh surface. Thus, the following proposition is needed for this purpose.

Proposition 3.1 *At any internal point of a developable piecewise linear surface, the summed inner angle is identically* 2π.

Proof For a point q_i on a developable piecewise linear surface patch M, if θ_j is an inner angle adjacent to q_i before flattening and θ_j^F is the corresponding inner angle flattened on the 2D plane, as illustrated in Fig. 3, the inner angles satisfy $\theta_j = \theta_j^F$ since the surface at this point can be flattened without stretching or overlapping. In the 2D plane, $\sum_j \theta_j^F$ equals 2π for an internal vertex. When M is developable, which demands $\theta_j = \theta_j^F$ at every point on M, we have $\sum_j \theta_j = 2\pi$.

The approximation Gaussian curvature formula in [41] on an internal triangular node q_i is

$$\kappa_{q_i} = \frac{2\pi - \sum_j \theta_j}{\frac{1}{3}\sum_j A_j}, \tag{1}$$

where θ_j are the inner angles incidental at q_i, and A_j are the corresponding triangle areas. When utilizing the above approximation of Gaussian curvature to detect the developability of the given patch M, by the theorem of differential geometry, we have $\kappa_{q_i} = 0$, which also leads to $\sum_j \theta_j = 2\pi$. □

For an internal vertex, we call it a *developable point* when $\sum_j \theta_j = 2\pi$ is satisfied at this point. Otherwise, it is called a *non-developable point*. Using Proposition 3-1, we can detect whether a given mesh patch M is developable by checking every internal vertex. However, simply stating whether a surface is developable or not is insufficient for identifying the degree of developability of the surface. Thus, we define the *developability function* on a tessellated surface as follows.

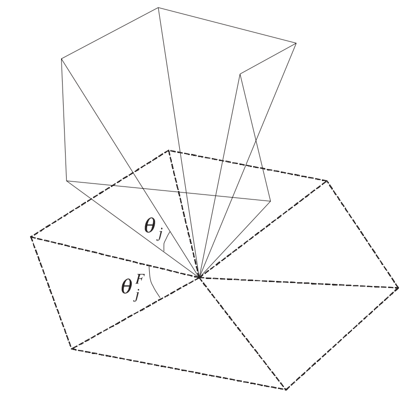

Fig. 3. The inner angles before and after flattening the triangles around a vertex

Definition 3.2 *The developability function of a tessellated surface M is defined as*

$$D[M] = \frac{1}{A}\sum\nolimits_i \delta(2\pi - \theta_{sum}(q_i))A_{q_i} \tag{2}$$

where $\delta(t)$ is the impulse function, $A_{q_i} = \frac{1}{3}\sum_j A_j$ is the sum of the areas of the incidental triangles at a vertex q_i on M, and A is the area of M. $\theta_{sum}(q_i)$ is either the sum of inner angles incidental at q_i when q_i is an internal vertex, or set to 2π if q_i is on the boundary of M.

The developability function is actually a weighted sum of the discrete Gaussian curvature given in Eq. 1. The value of the developability function gives a progressive estimate of the developability of a surface. When $D[M] = 1$, all internal vertices on this surface are developable points; in other words, M is developable. When $D[M] = 0$, it means that we cannot find any developable point on the surface; M is absolutely non-developable. For any $D[M] \in (0,\ 1)$, there are some developable points on M. The larger the value of $D[M]$, the more developable the surface M is.

3.3 Constrained optimization

For a given polygonal patch M with n vertices and $D[M] < 1$, the problem we have to solve here is to find an optimized $M*$ with the same topology as M but with different vertex positions. The $M*$ should be developable (i.e., $D[M*] = 1$), and the difference between $M*$ and M should be minimized since the shape of M is what the designer desires. Therefore, we formulate the problem as a *constrained optimization problem*

$$\min(M - M*) \text{ subject to } D[M*] = 1. \tag{3}$$

In the definition of the developability function, there is an impulse function that may lead to irregularity during the optimization. Here, we define a new *developability detect function* to take place of the developability function $D[\cdots]$ as

$$G[M*] = \sum\nolimits_i (g(q_i(M*)))^2 \tag{4}$$

where $q_i(M*)$ is the position of a triangular vertex $q_i \in M*$, and the function is the *vertex developability detect function* given as

$$g(q_i) = \begin{cases} 2\pi - \sum_k \theta_k & (q_i \notin B) \\ 0 & (q_i \in B) \end{cases} \tag{5}$$

where B is the set of triangular vertices on the boundary of the given mesh patch $M*$. It is not hard to verify that when $G[M*] = 0$, the sum of the inner angles at every internal vertex equals 2π, hence $D[M*] = 1$ is satisfied. Thus, we replace the developability constraint by this new one and the constrained optimization problem is redefined as

$$\min(M - M*) \text{ subject to } G[M*] = 0. \tag{6}$$

It is important to state that the optimization formulation of Eq. 6 pertains to a single patch M_i on the embedded object O. Since O is usually made of several surface patches assembled together, the continuity constraint should also be added when these patches are optimized individually. This will be discussed when the details of the algorithm are presented.

4 Global optimization

A penalty-function-based scheme is presented in this section that solves the constrained optimization problem of Eq. 6. This is a global optimization (i.e., all vertices move at the same time at an iteration step). Two essential tasks need to be embarked upon: the numerical solution of the optimization itself and the continuity preservation among the patches during the optimization process, as entailed separately next.

4.1 Penalty-function-based scheme

By definition of the constrained optimization problem (Eq. 6), we attempt to minimize the surface discrepancy between M and $M*$. An elastic energy $E(M*)$ is defined below to quantify the difference,

$$E(M*) = \sum_j (\|q_{j,s}q_{j,e}\| - l_j^0)^2 \tag{7}$$

where j is the index of a triangular edge, $q_{j,s} \in M*$ and $q_{j,e} \in M*$ are the vertices of the edge, and l_j^0 is the length of the triangular edge j on M. This energy function simulates a spring network in which every spring follows along a triangular edge on $M*$. The energy measures the change of length on every triangular edge between $M*$ and M. Thus, the constrained optimization problem is redefined as

$$\min E(M*) \text{ subject to } G[M*] = 0. \tag{8}$$

Equation 8 can be converted into an unconstrained optimization problem by adding the constraint as a penalty term to the objective function [45]. As a result, the objective function to be optimized becomes

$$J(M*) = E(M*) + \frac{\rho}{2}(G(M*))^2 \tag{9}$$

where ρ is the coefficient to balance the weight between $E(M*)$ and $G(M*)$. The choice of ρ is by no means trivial. For a smaller ρ, the computing procedure converges slowly to $G[M*] = 0$. When ρ is large, on the other hand, the shape of the surface after optimization usually deviates too much from the one before the optimization. For any starting optimization point M^0, the procedure begins to minimize $J(M^0)$ with $\rho = \frac{1}{n_e(G[M^0])^2}\sum_j (l_j^0)^2$, where n_e is the number of triangular edges. After applying the conjugate gradient method to minimize the value of $J(M)$ with a fixed number of iteration steps (which is empirical and is five in our implementation), we obtain a new point M^1. Then, we use M^1 as a starting guess for the minimum of $J(M)$ with $\rho = \frac{1}{n_e(G[M^1])^2}\sum_j (l_j^0)^2$ and obtain M^2, and so on. In actual computation, we stop the process either when the constraint violation is less than a given threshold or when changes in $J(M)$become insignificant.

This optimization procedure guarantees the convergence. Since our objective function (Eq. 9) is in a quadratic form, with a fixed ρ, the conjugate gradient procedure will converge to a minimum near the initial value. This follows what we expected to minimize the difference of M and $M*$. With the value of $G[M^i]$ becomes smaller and smaller, ρ increases accordingly, so the surface evolves to be more and more developable during the computing (i.e., $G[M] \to 0$). Theoretically, we arrive at the developable patch $M*$ in the limit as ρ tends to infinity.

When using the gradient-based method to minimize $J(M)$, we need to compute the gradients of J with respect to q_i. First of all, we have

$$\frac{\partial J}{\partial q_i} = \frac{\partial E}{\partial q_i} + \rho G \frac{\partial G}{\partial q_i}. \tag{10}$$

Analytically, $\frac{\partial E}{\partial q_i} = \frac{\partial}{\partial q_i}\sum_j (\|q_i q_j\| - l_{ij}^0)^2$, where q_j are the vertices adjacent to q_i, and l_{ij}^0 are the original length between q_i and q_j. Thus, we obtain

$$\frac{\partial E}{\partial q_i} = \sum_j 2(\|q_i q_j\| - l_{ij}^0)\frac{q_j - q_i}{\|q_j q_i\|}. \tag{11}$$

For $\frac{\partial G}{\partial q_i}$, since it is very complex (with more than 40 terms), we compute it numerically using the central difference equation $\frac{\partial G}{\partial q_i} = \frac{G(q_i+h)-G(q_i-h)}{2h}$. When the position of a vertex q_i is changed, of all the terms in G, only the $g(\cdots)$s with respect to q_i and its adjacencies will incur changes. Thus, to reduce the computing time of $\frac{\partial G}{\partial q_i}$, we adopt the following equation to determine it numerically,

$$\frac{\partial G}{\partial q_i} = \frac{G_P(q_i+h) - G_P(q_i-h)}{2h}, \tag{12}$$

where $G_P(q_i) = (g(q_i))^2 + \sum_j (g(q_j))^2$ with q_j being the adjacent vertices to q_i, and h is a small constant (the determination method of h according to the value of $G_P(q_i)$ is from [46]).

In the above formulas, the gradients of J with respect to the vertex positions of M are computed locally, so the computing time is reduced. Now, we can compute the optimized J with respect to M by a conjugate gradient method which includes the iterative process of computing gradients at current state and searching for an optimum state along the conjugate direction [45]. The unnecessary details of the conjugate gradient method are omitted here. The terminal condition of the conjugate gradient method is chosen to be $\frac{\|G[M^i]-G[M^{i-1}]\|}{G[M^0]} < \eta$ where $G[M^i]$ is the value of the constraint function in the ith iteration (current value), $G[M^0]$ is the value of the constraint function before optimization, and η is a small threshold number (we choose in our testing examples). Similar to other iterative solutions, a maximum iteration number is used in our system as another stop criterion – the numerical iteration stops after it has iterated steps.

4.2 Continuity preservation

In the object O consisting of assembled mesh patches M_i $(i = 1, \cdots, m)$, a vertex shared by more than one patches is called an *assembling vertex*. All other assembly constraints, e.g., different kinds of fixed tolerance, need to be converted into the information of coincident assembling vertices and their related linked vertex sets. Associated with an assembling vertex q_p, we define a *linked vertex set* L_{q_p}that contains all the mesh vertices in O coincidental at q_p. Also, for any vertex $q_q \in L_{q_p}$, there is the associated linked vertex set L_{q_q} where we have $q_p \in L_{q_q}$. The cardinality of the linked vertex set of a vertex is exactly the number of patches sharing the vertex. By means of these linked vertex sets, the connectivity information of assembled patches is stored. However, this connectivity is ignored when the shape of every $M_i \in O$ is being optimized individually – for two coincidental triangular nodes belonging to two different patches, their positions are adjusted independently since the gradients of J respect to them might be different; so cracks will appear at places where two patches originally met.

The numerical scheme then needs to be enhanced to take into consideration of preserving the G^0 continuity of O. The basic idea is to make the linked vertices consistent during the optimization. To achieve this consistency, the formulas of computing gradients at the assembling vertices are modified. When changing the position of an assembling vertex q_a, the positions of vertices in L_{q_a} should be maintained the same as q_a. Thus, the gradient of E with respect to q_a relates not only to $\sum (\|q_a q_j\| - l^0_{aj})^2$ but also all the other terms $\sum (\|q_p q_q\| - l^0_{pq})^2$ $(q_q \in L_{q_a})$ in E, where $q_a q_j$ are the incident edges at q_a, and $q_p q_q$ are the edges with one endpoint $q_q \in L_{q_a}$. Thus, the gradient is modified to become

$$\frac{\partial E}{\partial q_a} = \frac{\partial}{\partial q_a} \sum_j (\|q_a q_j\| - l^0_{aj})^2 = \sum_j 2(\|q_a q_j\| - l^0_{aj}) \frac{q_j - q_a}{\|q_j q_a\|}, \tag{13}$$

where q_j are either the vertices adjacent to q_a or the adjacent vertices to a vertex in L_{q_a}. Also, the gradient of G with respect to q_a should be changed to

$$\frac{\partial G}{\partial q_a} = \frac{G_{PA}(q_a + h) - G_{PA}(q_a - h)}{2h}, \tag{14}$$

where $G_{PA}(q_a) = (g(q_a))^2 + \sum_q (g(q_q))^2 + \sum_j (g(q_j))^2$ with q_j being either the adjacent vertices of q_a or the adjacent vertices ofq_q $(q_q \in L_{q_a})$. When calculated with the above prescribed method, the gradients of the linked vertices become consistent with each other. Therefore, while searching for the optimum along the conjugate direction, the updating of their positions is also kept consistent, which in turn ensures the G^0 continuity.

5 Local optimization

Although the penalty-function-based global optimization gives a high quality result, its computing speed is usually very slow and cannot satisfy the requirement of real-time design activities. In this section, the developability-by-deformation problem is reformulated as a local optimization problem and an algorithm is given that iteratively updates the position of vertices to achieve a developable mesh.

5.1 Reformulation of the problem

Recall the original definition of the constrained optimization problem (Eq. 6), our objective is to modify a given mesh M into a developable one $M*$, while minimizing the difference between M and $M*$. Let us consider only one vertex on the given mesh M, where $g(q) \neq 0$. The basic idea of local optimization is moving q along its normal direction n_q (which is the average normal of q's adjacent faces) to find a new position $q* = q + \delta n_q$ with $g(q*) = 0$; at the same time, the movement scale must be kept as small as possible in order to minimize the surface change. Therefore, the global optimization problem is decomposed into a combination of local optimizations on triangular vertices. On a vertex q, the problem is defined as

$$\min \delta^2 \text{ subject to } T(\delta) = 0, \tag{15}$$

with $T(\delta) = (g(q + \delta n_q))^2 + \sum_j (g(q_j))^2$ with q_j being the adjacent vertices to q_i. When q moves, it

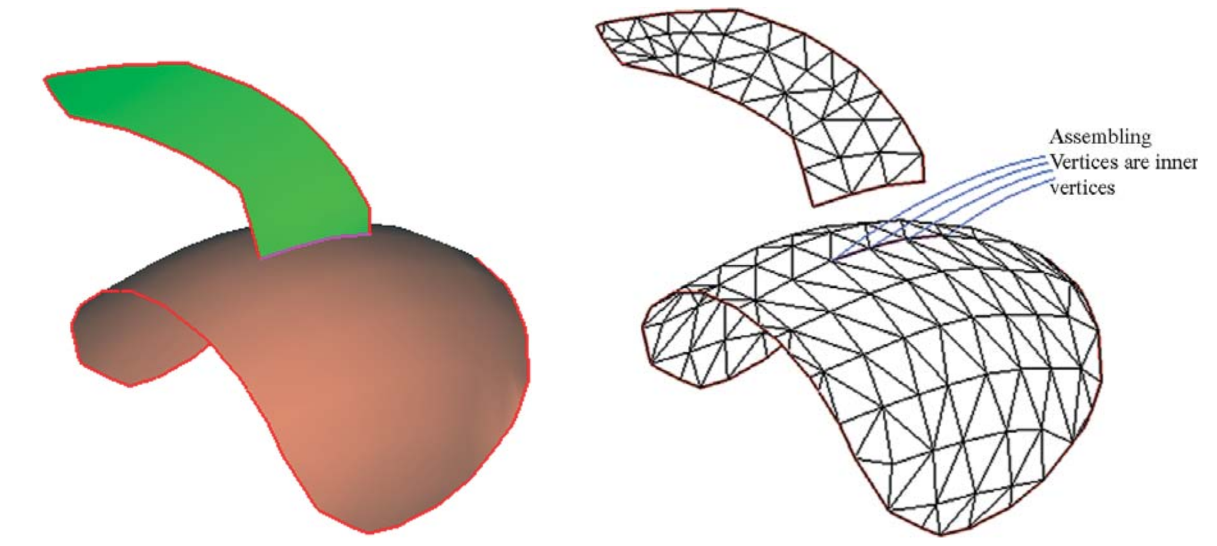

Fig. 4. Interior assembling vertices

affects not only the developability at q itself, but also that of all its adjacent vertices. Thus, the constraint $T(\delta)$ of local optimization on q is set on both the vertex q and its neighbors. When using the *Lagrange multiplier method* to solve the above optimization problem (Eq. 15), the Lagrange function can be written as

$$L = \delta^2 + \lambda T(\delta) \,, \tag{16}$$

where λ is the Lagrange multiplier. By setting $\frac{\partial L}{\partial \delta} = 0$ and $\frac{\partial L}{\partial \lambda} = 0$, we obtain the following equations:

$$2\delta + \lambda \frac{dT}{d\delta} = 0, \tag{17}$$

$$T(\delta) = 0. \tag{18}$$

After replacing $T(\delta)$ in Eq. 18 with a linear approximation based on T's Taylor series

$$T(\delta) \approx T(\delta_0) + \dot{T}(\delta_0)(\delta - \delta_0),$$

the following equation of updating is obtained

$$\delta = \delta_0 - \frac{T(\delta_0)}{\dot{T}(\delta_0)} \,. \tag{19}$$

From Eq. 17, we have $\lambda = -\frac{2\delta}{\dot{T}(\delta)}$, so by the property of the Lagrange method of constrained optimization [45], if $\delta \neq 0$ and $\dot{T}(\delta) \neq 0$, the iteration of Eq. 19 converges to the minimum (if $\dot{T}(\delta) = 0$, we just simply fix the vertex). Now that the magnitude of the update of an individual vertex at an iteration step is decided by Eq. 19, we next need a mechanism by which the order of the local optimization on the vertices can be determined. The square of the vertex developability detect function as defined in Eq. 5 presents itself to be a natural choice and is adopted in our system.

5.2 Outline of the algorithm

Our local optimization algorithm is built around vertex selection and vertex position updating. As mentioned earlier in Sect. 3.1, our system represents a model by an adjacency graph structure, which includes vertices, edges, and faces, as well as the connection relationship among them; they are all explicitly represented and linked together. Each vertex maintains a list of the edges of which it is a member. The overall algorithm is outlined below by *Algorithm* **LocalDevelopabilityOptimize**(O).

Algorithm **LocalDevelopabilityOptimize**(O)
Input: A given object O represented as a set
    of polygonal mesh patches
Output: The optimized polygonal mesh patches

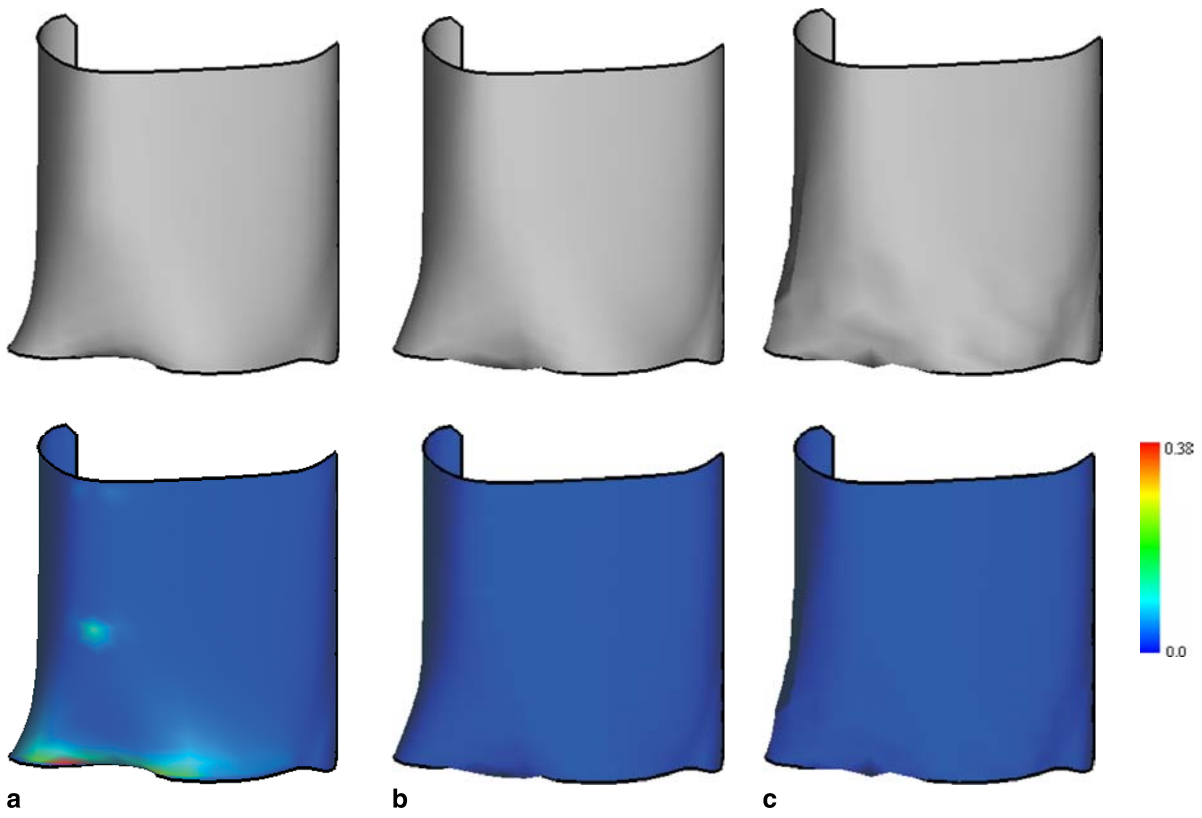

Fig. 5a–c. Example I. Global vs. local optimization: **a** Given surface and its Gaussian map **b** Results of global optimization **c** Results of local optimization ($\delta_T = 1.0$)

```
1.  Compute the vertex developability detect
    function $g(q)$ at each vertex $q$on the given
    mesh patches;
2.  Compute the unit normal $\boldsymbol{n}$ of each
    vertex $q$ on $O$;
3.  Place all vertices in a maximum heap $H$
    keyed on the $[g(\cdots)]^2$ measure –
    the vertex with the maximum $[g(\cdots)]^2$
    is placed at the top of $H$;
4.  4 ← 0;
5.  **Do** {
6.      Select the vertex $q$ at the top of $H$ and
        update its movement scale along its unit
        normal $\boldsymbol{n}$ according to Eq. 17;
7.      Update the cost of $q$ and its adjacent
        vertices to reflect the movement on $q$
        – this will change the locations of these
        vertices in $H$;
8.      $j \leftarrow j+1$;
9.  } **while** ((the of the vertex at top of $H$ is
    greater than $\varepsilon$) **and** ($j < N_{\max}$));
10. Update the positions of all the vertices
    by their movement scales;
11. Update the normal vectors of all the vertices
    on $O$;
12. **return**.
```

We elaborate the above algorithm by addressing the following questions.

5.2.1 Surface difference control

In the above algorithm, the difference between the optimized mesh and the given mesh is not controlled. Such a control can be added when updating the vertex q at the top of H – in our implementation, we just simply set $\delta = \delta_T$ if $\delta > \delta_T$ and truncate δ to $-\delta_T$ when $\delta < -\delta_T$, where δ_T is the given difference tolerance. It calls to pay special attention to the unit

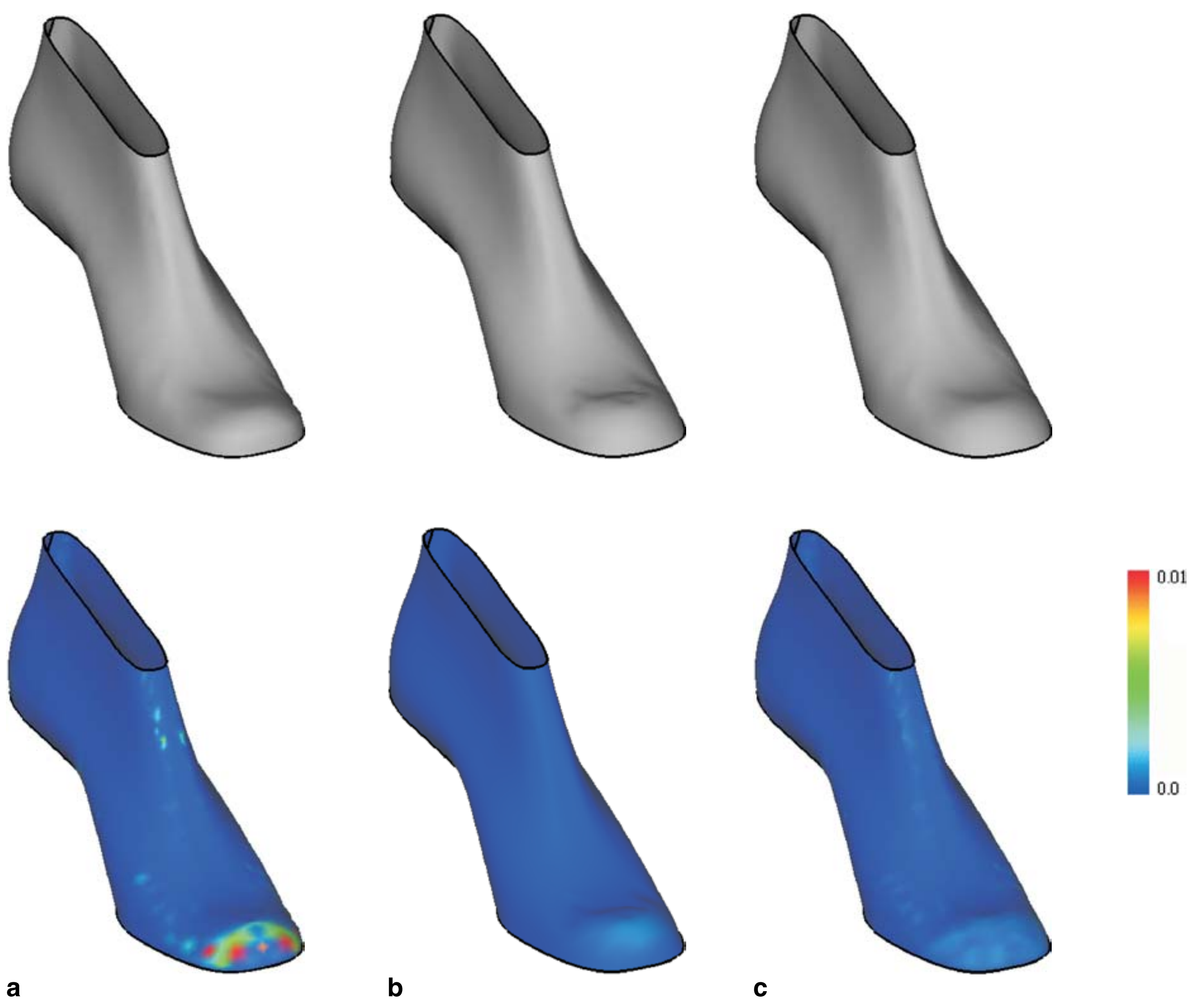

Fig. 6a–c. Example II. The surface of a shoe last: **a** Given surface and its Gaussian map **b** Result of global optimization **c** Result of local optimization ($\delta_T = 0.38$)

normal at each vertex – it remains unchanged in the entire iterative process and is updated only once at the end of the process – every vertex moves along its original normal passing through its original position during the iteration. If all vertices move by δ_T along their original normal directions, the result would be identical to an offset surface of the given surface (δ_T is the value of offset). Therefore, the optimized mesh is controlled between the $+\delta_T$ and $-\delta_T$ offset surfaces of the given surface. The smaller the tolerance δ_T, the closer the optimized mesh patches are to the original surface, and the slower the optimization algorithm converges. On the other hand, a larger tolerance δ_T will result in a faster convergence but at a cost of larger deviation from the original surface.

5.2.2 Terminal conditions of iterations

During the iteration of algorithm **LocalDevelopabilityOptimize**(O), the value of the vertex at top of the heap decreases while the step number of iteration, j, increases. These two factors are utilized to control the terminal condition of the iteration. Which of the two takes effect depends crucially on the given tolerance δ_T. When the value of δ_T is large enough, the

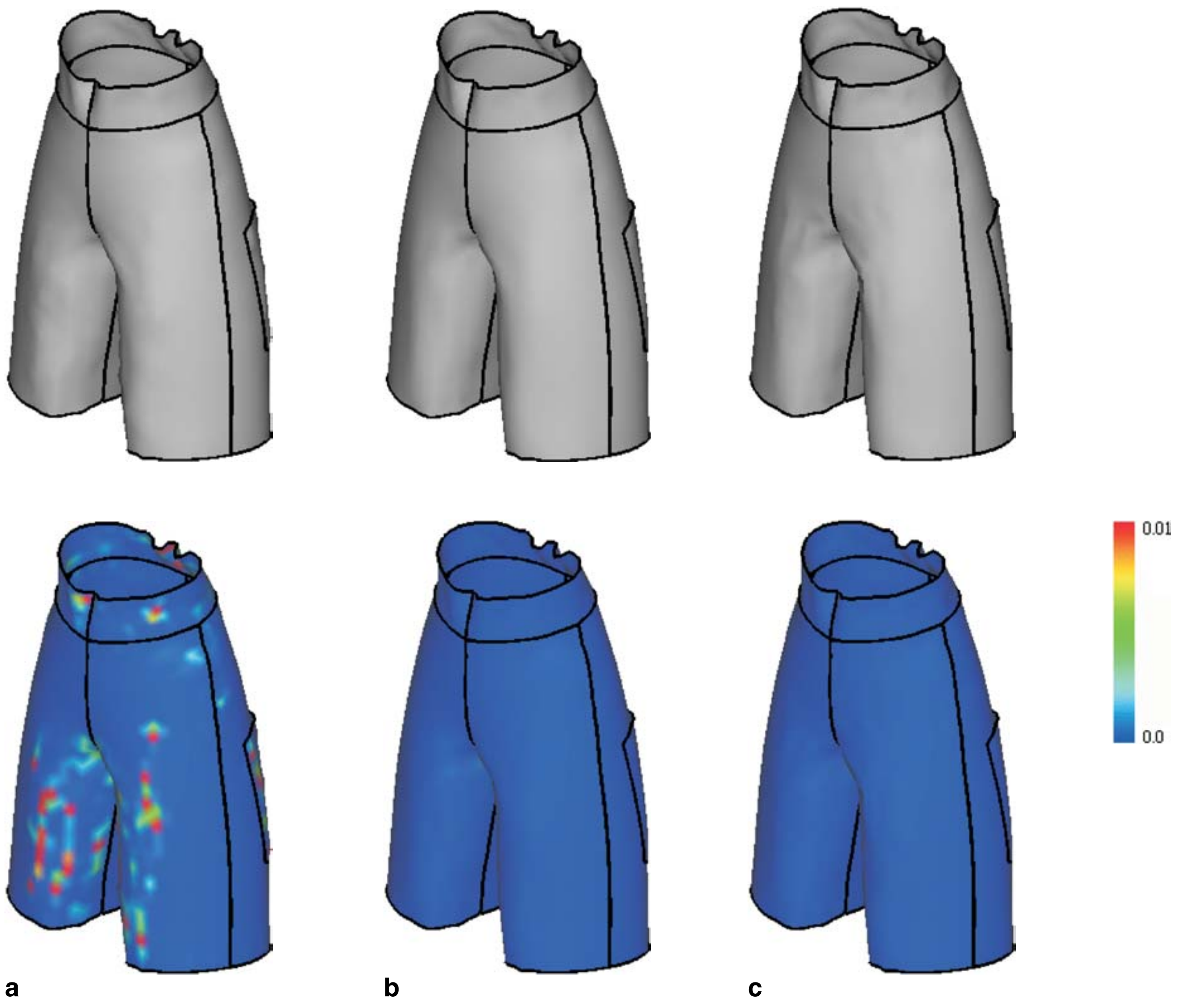

Fig. 7a–c. Example III. A pair of short pants with multiple patches: **a** The original pants and their Gaussian map **b** Result of global optimization **c** Result of local optimization ($\delta_T = 2.4$)

given polygonal patches can be fully optimized, we stop at $g(q) \le \varepsilon$ for the top element q in heap H. On the other hand, a δ_T that is too small will stingingly limit the movement of each vertex and the optimization (Eq. 15) would dwell at certain level and has to be stopped by the maximum number of iterations criterion.

5.2.3 Continuity preservation

By definition, the value of any point on the boundary of O is zero; as a result, it will not be moved during the optimization (note that a vertex with zero $[g(\cdots)]^2$ is put at the bottom of heap H). However, one still faces the continuity problem if an assembling vertex is interior to some patch (see Fig. 4). We resolve this problem in the simplest way – all the assembling vertices remain fixed during the optimizing process. For an interior assembling vertex, if its $[g(\cdots)]^2 > 0$, its developability is enhanced via adjusting the positions of its adjacent vertices. The reason why the developability at an internal assembling vertex can be achieved by perturbing the neighboring non-assembling vertices, is that by the definition of function $T(\delta)$ in

Table 1. Computational statistics

Example	Vertex number	Optimize approach	Time cost	Result figure	$g^0_{\max}$	$g^*_{\max}$	Terminal condition
I	517	Global	46s	Fig. 5b	0.14	2.1×10^{-3}	$\frac{\left\|G[M^i]-G[M^{i-1}]\right\|}{G[M^0]} \le 0.01\%$
		Local	1s	Fig. 5c		9.9×10^{-5}	$g^*_{\max} \le 10^{-4}$
II	3047	Global	390s	Fig. 6b	0.093	1.1×10^{-3}	$N_{\max} = 200$
		Local	23s	Fig. 6c		1.0×10^{-3}	
III	3016	global	310s	Fig. 7b	0.19	1.3×10^{-3}	$N_{\max} = 200$
		local	1s	Fig. 7c		9.9×10^{-5}	

* All tested on a P III 900 PC with a program written in C++ with (1) $\eta = 0.01\%$ and $N_{\max} = 200$ for the global optimization approach and (2) $\varepsilon = 10^{-4}$ and $N_{\max} = 500\,000$ for the local optimization approach.

Eq. 15, $T(\delta) = (g(q+\delta n_q))^2 + \sum_j (g(q_j))^2$, where q_j are the adjacent vertices to the moved vertex, the movement of a vertex is not only a measurement of the developability at this vertex but also of the vertices around it. Therefore, when perturbing the non-assembling vertices around an assembling vertex, the developability at the assembling vertex is also increased.

6 Experimental results

In this section, we give some experimental examples to demonstrate the functionality of both the global and local optimization approaches, as well as a comparison. In the first example, Example I, which was originally shown in Fig. 1, we applied both the global and local optimizations to the original surface. The surface before optimization and its Gaussian map are given in Fig. 5a (in a Gaussian map, the color of a point represents its $[g(\cdots)]^2$ value). The resultant surfaces after both the global and local optimizations are shown in Fig. 5b and 5c, respectively, where for the local optimization of Fig. 5c the tolerance δ_T is set to 1.0. Both the global and local optimization approaches achieve fully optimized results within the required maximum iteration steps. As seen in the figures, the global optimization gives a smoother resultant surface. This is because in a global optimization all the vertices move together, while the local approach moves vertices one by one. Therefore, the original smoothness of the given surface is not maintained by the local optimization approach. The following examples, Example II and III, also verify this point.

Example II is the surface of a shoe upper layer. Since it is usually manufactured from a planar leather sheet, the surface is desired to be developable. Figure 6 displays the optimization results. In this particular case, neither the global nor the local approach can achieve the full optimum, i.e., both of them were stopped by the maximum iteration step criterion (for the local optimization the difference tolerance δ_T is set to 0.38).

Example III comes from the application of apparel industry. The assembled polygonal patches of a pair of short pants are constructed in three-dimensional space. Each patch must be developable since it will come from its corresponding 2D pattern in manufacturing. The Gaussian map of the original surface (Fig. 7a) shows that the original design incurs severe non-developability. The result surfaces after the optimizations are shown in Fig. 7b and 7c. Unlike the first two examples, in this case, the local optimization approach, with $\delta_T = 2.4$, achieves a fully developable result while the global approach fails to do so within 200 iteration steps.

The computational statistics of Example I, II, and III are given in Table 1. Implemented by a program written in C++ and running on a standard PC, the local optimization approach is seen to be able to generate the desired result in near real-time. On the other hand, the global optimization approach usually takes several minutes to reach a result with a decent level of surface developability. As expected, the converge speed of the local optimization crucially depends on the difference tolerance . For a properly chosen δ_T, the local optimization can converge quickly. Otherwise, the iterative process is stopped by the maximum iteration

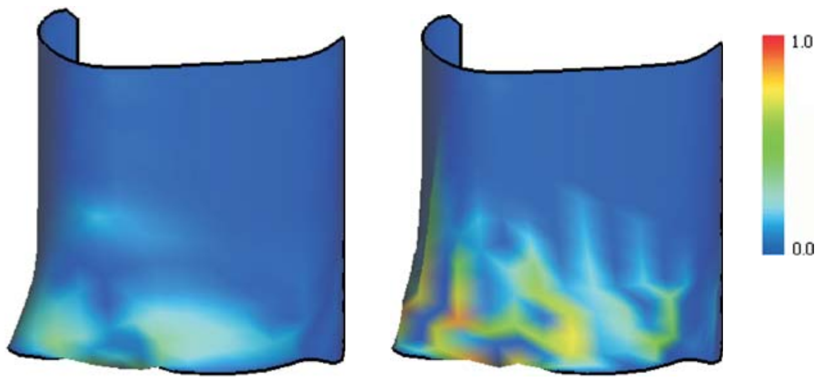

a

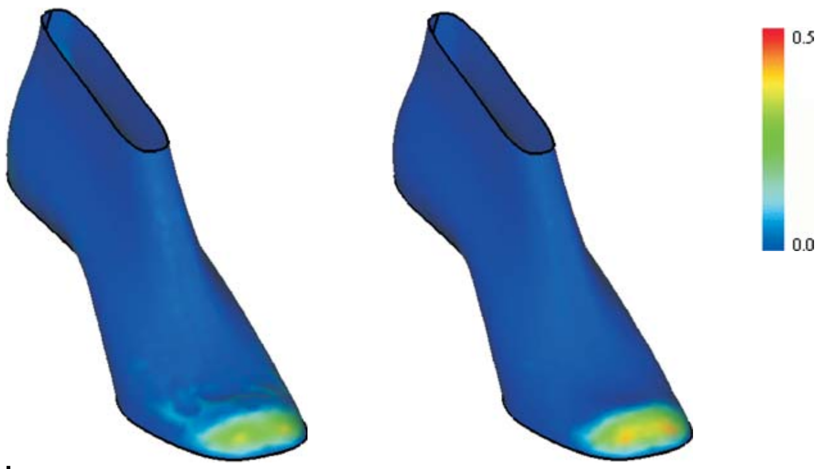

b

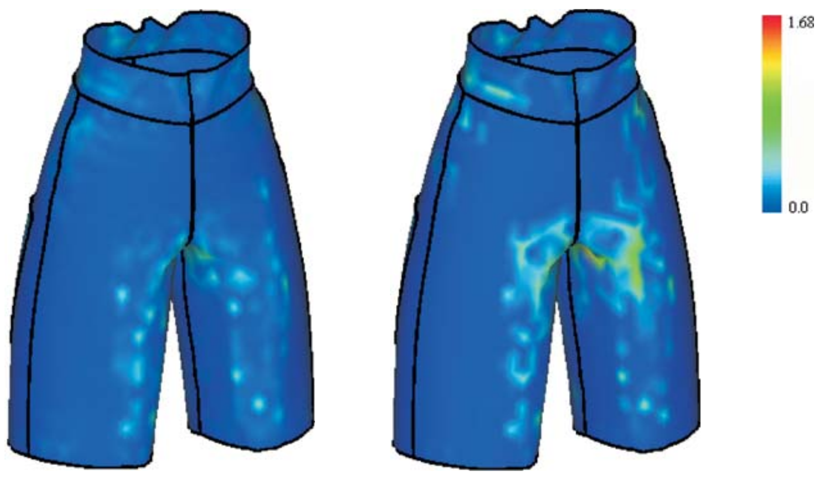

c

Fig. 8a–c. The distance error maps of global and local optimization results: **a** Example I **b** Example II **c** Example III

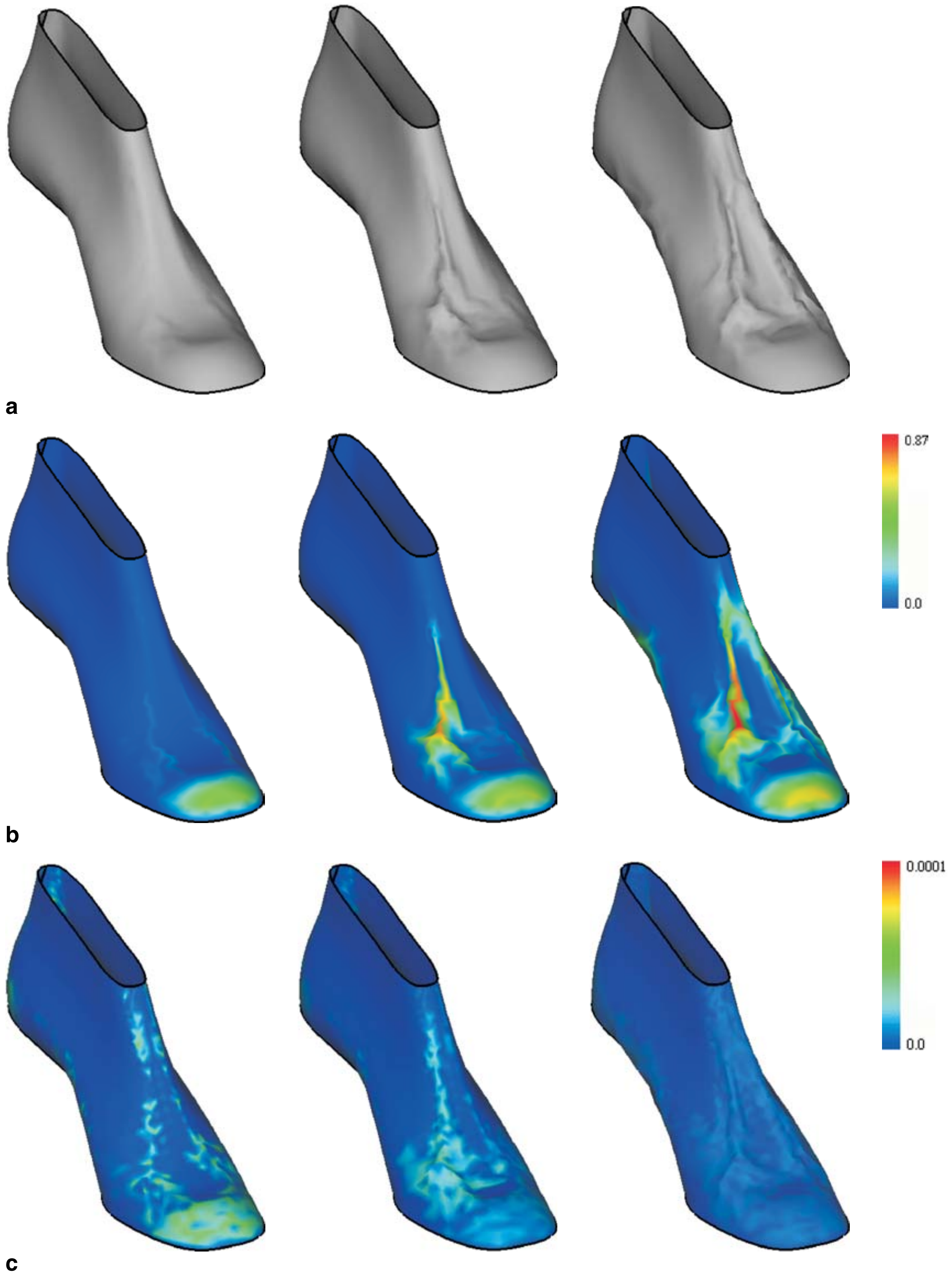

Fig. 9a–c. Increasing δ_T leads to larger distance errors but better developability: **a** Resultant surfaces **b** Distance error maps of the resultant surfaces **c** Gaussian maps of the resultant surfaces

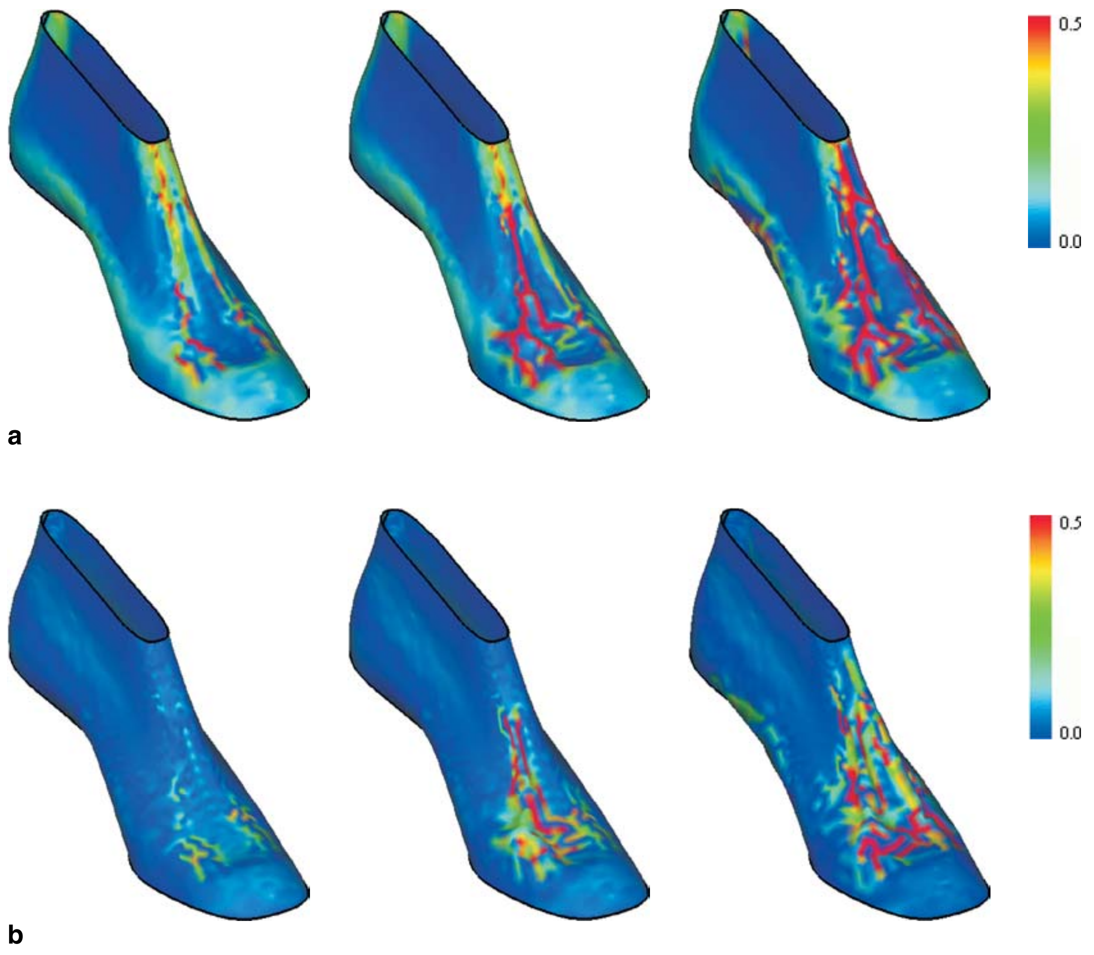

Fig. 10a,b. Increasing δ_T leads to more wrinkles (larger principal curvature) but better developability: **a** $|\kappa_{\min}|$ of the resultant surfaces **b** $|\kappa_{\max}|$ of the resultant surfaces

criterion $N_{\max}$. In the most extreme case of $\delta_T = 0$, no improvement can be made as the original surface is fixed. After experimenting with a variety of test examples, it is observed that a $\delta_T = \bar{L}$, in general, achieves satisfactory improved developability while maintaining reasonably well the dimensions of the original surface, where $\bar{L}$ is the average length of the triangular edges on the given polygonal mesh patches. Thus, in all three examples, δ_T is set to be $\bar{L}$.

In addition to the Gaussian map, the *distance error map*, in which the colors represent the distances of vertices to the original surface, is utilized in our system to compare the results from global and local approaches. The distance error maps for the given three examples are shown in Fig. 8. As revealed from the figure, the maximum distance error from the global optimization approach is generally smaller than the one generated from the local approach. This phenomenon can be explained by noting that, by its nature, in the local optimization, only a small subset of the vertices with high $[g(\cdots)]^2$ values will be moved, whereas in the global optimization all the vertices are moved in sync at each iteration step. As a result, to achieve the same level of overall developability, certain vertices often need to be moved by larger distances in the local optimization than their counterparts in the global optimization, due to the restraint on the moveable vertices in the local optimization.

The distance error map is also adopted to study the effect of the difference tolerance δ_T on the level of optimization in the local optimization approach. In Fig. 9, it is evidently seen that enlarging δ_T increases the freedom of movement for vertices in the local optimization which in turn enhances the optimization result. Viewed from another perspective, the distance error map together with the Gaussian map of the final optimized surface serve to "measure" the level of non-developability of the original surface. Smaller errors on the distance error map but larger values on the Gaussian map indicate an "easy" conversion from the original non-developable surface to a highly developable surface with minimum deviation, while the opposite combination implies a "difficult" task. Large discrepancies result on the final surface if a high degree of developability is desired. The maps of principal curvatures $|\kappa_{\min}|$ and $|\kappa_{\max}|$ of the surfaces in Fig. 9 are also listed in Fig. 10. It is easy to find that the principal curvatures are increased with the enlargement of δ_T, so more wrinkles occur. However, for example when $\delta_T = 1.0$, the places with large $|\kappa_{\min}|$ have a corresponding small value of $|\kappa_{\max}|$ (see Fig. 10). That's why more wrinkles can still give a result with better developability.

7 Summary and discussion

The focus of this paper is the so called developability-by-deformation problem: How to deform a given non-developable polygonal surface into a developable one with minimum change. Because developability of a surface is often a strongly required attribute in a diversity of engineering applications, a practical solution to this problem is highly needed. We contribute by proposing two numerical solutions to the developability-by-deformation problem. Both approaches are based on the principle of energy minimization, which seeks to minimize the amount of deformation while at the same time maximizes the degree of developability of the surface. The two differ with each other in how this minimization is formulated as well as the way the vertices on the polygonal mesh are moved during the minimization process: while the first approach formulates the minimization as a global constrained optimization in which all the vertices move simultaneously at each iteration step, the second approach is of local optimization nature where only one vertex is moved at a time based on a locally defined optimization criterion. Experimental examples are provided to demonstrate the functionality of the proposed two approaches as well as their comparison in terms of computing cost, effectiveness of attaining developability, dimensional difference between the surfaces before and after the optimization, and other important aspects.

Both solutions can be integrated into a geometric modeling system for product design where surface developability is obliged. Owing to its better ability of maintaining the smoothness of the original surface due to its global nature, the first solution, the global optimization approach, can be used for those applications where the smoothness and quality of the product surface are emphasized. On the other hand, the local optimization based solution may better suit situations where real-time computation – such as in computer graphics simulation – is demanded. Another potential application of the local optimization solution is in wrinkle design, such as in shoe manufacturing, where wrinkles are sometimes deliberately designed to be formed during the manufacturing process of the shoe (for fashion and aesthetic purposes).

For possible future work, as mentioned above, since the smoothness of the original surface is not preserved during the local optimization, one potential topic is how to add smoothing terms into the local updating operator to enforce the required smoothness on the surface. Also, in our current implementation of the local optimization, the surface continuity of multiple patches is preserved by simply fixing all the assembling vertices during the optimizing iteration – this obviously limits the degree of freedom of vertex movements. Thus, studying a better and more flexible continuity preserving method in the local optimization approach is another item worthy of further research. The topology of the original polygonal surface can be preserved by enforcing continuity across the boundaries of triangular patches. However, self-intersection might occur after repositioning the vertices, especially in the case of the local optimization with large δ_T. Another possibility for further work is thus to integrate the self-collision detection and responding algorithm into the strategy of vertex movement.

References

1. do Carmo MP (1976) Differential geometry of curves and surfaces. Prentice-Hall, Englewood Cliffs, NJ
2. Singh K, Fiume E (1998) Wires: a geometric deformation technique. SIGGRAPH 1998 Conference Proceedings, ACM, pp 405–414
3. Schroeder WJ, Zarge JA, Lorensen WE (1992) Decimation of triangle meshes. Comput Graph 26(2):65–70
4. Garland M, Heckbert PS (1997) Surface simplification using quadric error metrics. SIGGRAPH 97 Conference Proceedings, pp 209–16
5. Wu J-H, Hu S-M, Tai C-L, Sun J-G (2001) An effective feature-preserving mesh simplification scheme based on face constriction. Proceedings of the Ninth Pacific Conference on Computer Graphics and Applications, Tokyo, 16–18 October 2001, pp 12–21
6. Taubin G (1995) A signal processing approach to fairing surface design. SIGGRAPH 95 Conference Proceedings, ACM, pp 351–58
7. Kobbelt L, Campagna S, Vorsatz J, Seidel HP (1998) Interactive multi-resolution modeling on arbitrary meshes. SIGGRAPH 98 Conference Proceedings, ACM, pp 105–114
8. Desbrun M, Meyer M, Schroder P, Barr AH (1999) Implicit fairing of irregular meshes using diffusion and curvature flow. SIGGRAPH 99 Proceedings, ACM, pp 409–416
9. Schneider R, Kobbelt L (2000) Generating fair meshes with G^1 boundary conditions. Proceedings Geometric Modeling and Processing 2000 Theory and Applications. IEEE Comput Soc 2000, pp 251–261, Los Alamitos, CA
10. Schneider R, Kobbelt L (2001) Geometric fairing of irregular meshes for free-form surface design. Comput Aided Geom Des 18(4):359–379
11. Zeleznik RC, Herndon KP, Hughes JF (1996) SKETCH: an interface for sketching 3D scenes. SIGGRAPH 96 Proceedings, ACM, pp 163–170
12. Igarashi T, Matsuoka S, Tanaka H (1999) Teddy: a sketching interface for 3D freeform design. SIGGRAPH 99 Proceedings, ACM, pp 409–416
13. Bloomenthal J, Wyvill B (1990) Interactive techniques for implicit modeling. 1990 Symposium on Interactive 3D Graphics, pp 109–116
14. Markosian L, Cohen J M, Crulli T, Hughes J (1999) Skin: a constructive approach to modeling free-form shapes. SIGGRAPH 99 Conference Proceedings, ACM, pp 393–400
15. Suzuki H, Sakurai Y, Kanai T, Kimura F (2000) Interactive mesh dragging with an adaptive remeshing technique. Vis Comput 16(3–4):159–76
16. Zorin D, Schroder P, Sweldens W (1997), Interactive multiresolution mesh editing. SIGGRAPH 97 Proceedings, ACM, pp 259–268
17. Khodakovsky A, Schroder P (1999) Fine level feature editing for subdivision surfaces. Proceedings Fifth Symposium on Solid Modeling and Applications. ACM Press, New York, pp 203–211
18. Aumann G (1991) Interpolation with developable Bézier patches. Comput Aided Geom Des 8:409–420
19. Maekawa T, Chalfant J (1998) Design and tessellation of B-spline developable surfaces. ASME Trans J Mech Des 120:453–461
20. Frey WH, Bindschadler D (1993) Computer aided design of a class of developable Bézier surfaces. GM Research Publication, GMR-8057
21. Chu CH, Séquin CH (2002) Developable Bézier patches: properties and design. Comput-Aided Des 34(7):511–527
22. Hoschek J, Pottmann H (1995) Interpolation and approximation with developable B-spline surfaces, In: Daehlen M, Lyche T, Schumaker LL (eds) Mathematical methods for curves and surfaces. Vanderbilt University Press, Nashville, TN, pp 255–264
23. Chen HY, Lee IK, Leopoldseder S, Pottmann H, Randrup T, Wallner J (1999) On surface approximation using developable surfaces. Graph Models Image Process 61(2):110–124
24. Pottmann H, Wallner J (1999) Approximation algorithms for developable surfaces. Comput Aided Geom Des 16(6):539–556
25. Redont P (1989) Representation and deformation of developable surfaces. Comput Aided Des 21(1):13–20
26. Randrup T (1998) Approximation of surfaces by cylinders. Comput Aided Des 30(7):807–812
27. Park FC, Yu J, Chun C (2002) Design of developable surfaces using optimal control. ASME Trans J Mech Des 124:602–608
28. Shimada T, Tada Y (1991) Approximate transformation of an arbitrary curved surface into a plane using dynamic programming. Comput Aided Des 23(2):155–159
29. Parida L, Mudur SP (1993) Constraint-satisfying planar development of complex surfaces. Comput Aided Des 25(3):225–232
30. McCartney J, Hinds BK, Seow BL (1999) The flattening of triangulated surfaces incorporating darts and gussets. Comput Aided Des 31(3):249–260
31. Wang CCL, Smith SSF, Yuen MMF (2002) Surface flattening based on energy model. Comput Aided Des 34(8):823–833
32. Yu G, Patrikalakis NM, Maekawa T (2000) Optimal development of doubly curved surfaces. Comput Aided Geom Des 17:545–577
33. Sheffer A, de Sturler E (2000) Parameterization of faceted surfaces for meshing using angle based flattening. Eng Comput 17(3):326–337
34. Sheffer A, de Sturler E (2002) Smoothing an overlay grid to minimize linear distortion in texture mapping. ACM Trans Graph 21(3):874–890
35. Azariadis PN, Aspragathos NA (2000) On using planar developments to perform texture mapping on arbitrarily curved surfaces. Comput Graph 24(4):539–554
36. Azariadis PN, Aspragathos NA (2001) Geodesic curvature preservation in surface flattening through constrained global optimization. Compu Aided Des 33(8):581–591
37. Azariadis PN, Nearchou A, Aspragathos NA (2002) An evolutionary algorithm for generating planar developments of arbitrarily curved surfaces. Comput Ind 47(3):357–368
38. Aono M, Denti P, Breen DE, Wozny MJ (1996) Fitting a woven cloth model to a curved surface: dart insertion. IEEE Comput Graph Appl 16(4):60–70
39. Aona M, Breen DE, Wozny MJ (2001) Modeling methods for the design of 3D broadcloth composite parts. Comput Aided Des 33(10):989–1007

40. Calladine CR (1986) Gaussian curvature and shell structures. In: Proceedings of Mathematics of Surfaces, pp 179–196, Oxford, UK, Conference Information: Manchester, UK, 17–19 Sept. 1984
41. Kobbelt LP, Bischoff S, Botsch M, Kähler K, Rössl C, Schneider R, Vorsatz J (2000) Geometric modeling based on polygonal meshes. EUROGRAPHICS 2000 Tutorial
42. Sheffer A (2002) Spanning tree seams for reducing parameterization distortion of triangulated surface. SMI 2002: International Conference on Shape Modelling and Applications, pp 261–272
43. Hoppe H, DeRose T, Duchamp T, McDonald J, Stuetzle W (1993) Mesh optimization, SIGGRAPH 93 Proceedings, ACM, pp 19–26
44. Ganapathy S, Dennehy TG (1982) A new general triangulation method for planar contours. Comput Graph 16(3):69–75
45. Belegundu AD, Chandrupatla TR (1999) Optimization concepts and applications in engineering. Prentice-Hall, Upper Saddle River, NJ
46. Moreton HP, Sequin CH (1992) Functional optimization for fair surface design. ACM Comput Graph 26(2):167–176

CHARLIE C.L. WANG is currently an assistant professor at the Department of Automation and Computer-Aided Engineering at the Chinese University of Hong Kong. He received his BEng (1998) in Mechatronics Engineering from the Huazhong University of Science and Technology, and his MPhil (2000) and PhD (2002) in Mechanical Engineering from the Hong Kong University of Science and Technology. His research interests include design automation and optimization, geometric modeling, reverse engineering, CAD/CAM, and computer graphics.

KAI TANG is currently a faculty member in the Department of Mechanical Engineering at Hong Kong University of Science and Technology. Before joining HKUST in 2001, he had worked for more than 13 years in the CAD/CAM and IT industries. His research interests concentrate on designing efficient and practical algorithms for solving real world computational, geometric, and numerical problems. Tang received his PhD in computer engineering from the University of Michigan in 1990, his MSc in information and control engineering in 1986 also from the University of Michigan, and his BSc in Mechanical Engineering from Nanjing Institute of Technology in China in 1982.